

# Low drug load high retention mometasone furoate cream with Polyglyceryl - 3 oleate as a chemical enhancer: formulation development, in vivo and in vitro evaluation and molecular mechanisms

**Wenxuan Jia**

Shenyang Pharmaceutical University

**Yu Pang**

Shenyang Pharmaceutical University

**Chenyu Zhao**

Shenyang Pharmaceutical University

**Yu Cai**

Shenyang Pharmaceutical University

**Yang Zhang**

Shenyang Pharmaceutical University

**Chao Liu**

Shenyang Pharmaceutical University

**Liang Fang** (✉ [fangliang2003@yahoo.com](mailto:fangliang2003@yahoo.com))

Shenyang Pharmaceutical University School of Pharmacy <https://orcid.org/0000-0001-9966-3880>

---

## Research Article

**Keywords:** mometasone furoate, O/W cream, polyglyceryl-3 oleate, release enhancement, retention enhancement, molecular interaction

**Posted Date:** October 11th, 2023

**DOI:** <https://doi.org/10.21203/rs.3.rs-3390900/v1>

**License:**   This work is licensed under a Creative Commons Attribution 4.0 International License.

[Read Full License](#)

---

# Abstract

In the present study, an oil-in-water (O/W) cream containing 0.05% mometasone furoate (MF) was prepared for the treatment of atopic dermatitis (AD) using Polyglyceryl-3 oleate (POCC) as a chemical enhancer. The cream formulation was screened by stability and *in vitro* skin retention studies and optimized by Box-Behnken design. Appearance, rheological and irritation were investigated. The formulations were evaluated by *in vivo* tissue distribution and pharmacodynamic experiments. The molecular mechanisms by which POCC increases MF release and skin retention were investigated using rheology, molecular simulation, tape stripping, CLSM, ATR-FTIR and SAXS. The optimized formulation contained 10% POCC. Its addition made the cream smoother, more fluid and non-irritating. It increased MF release by 1.77-fold and skin retention *in vivo* by 3.14-fold. It demonstrated a good therapeutic effect in a mouse model of chronic AD, with a 59.52% reduction in ear weight difference, with no significant difference compared to a commercial cream (Elocon<sup>®</sup>) with 0.1% MF. The incorporation of POCC decreased the cohesive energy density of the oil phase of the cream and increased the fluidity of the drug in the cream, which increased the release of MF. It disrupts the long-period phase of lipids in the stratum corneum of the skin and facilitates the entry of MF into the skin, while POCC forms hydrogen bonds with MF and collagen in the dermis, thereby increasing the retention time. This study demonstrated that POCC can be used as a chemical enhancer in creams, providing a reference for the development of semi-solid formulations.

## 1. Introduction

Atopic dermatitis (AD) is a chronic and recurrent inflammatory skin condition. The main features of AD include dry skin, persistent eczema-like lesions and intense itching (pruritus)[1]. Topical corticosteroids are widely recommended as the first-line anti-inflammatory treatment for AD, and their intermittent use carries minimal risk[2].

Mometasone furoate (MF) belongs to the class of moderately potent topical corticosteroids and is particularly suitable for conditions like atopic dermatitis, which exhibit high sensitivity to topical corticosteroid therapy [3]. The structural modifications of MF, including halogenation at the 9 $\alpha$ -position, substitution of the 21-OH group with chlorine, and esterification of the 17-OH group with furoate, significantly enhance its binding affinity to the corticosteroid receptor[4]. Clinical trials have demonstrated that mometasone furoate exhibits comparable or significantly superior efficacy to betamethasone in all indications for both adults and children, with a low risk of local and systemic adverse effects[5].

Currently available MF topical preparations used for treating AD consist of ointments, creams, gels and lotions. Commercial ointments contain white petroleum jelly and white beeswax, which are viscous and not well-suited for patient use due to their difficult application. The creams include dimethyl sulfoxide (DMSO) and sodium dodecyl sulfate (SDS), while ethanol is added to both the gel and lotion to increase solubility. MF has a high oil-water partition coefficient ( $\log P$  4.12) and poor water solubility. It was

deemed suitable for enhancing skin sensation and preventing irritation by dissolving it in the oil phase and subsequently distributing the oil phase into the aqueous phase to prepare an O/W cream.

A topical drug delivery system (TDS) involves administering medication to the skin surface or mucous membranes for the treatment of localized ailments. The main challenge for TDS is the ability of the drug/active ingredient to penetrate the skin through the stratum corneum barrier and remain in the skin without entering the bloodstream, thus avoiding systemic side effects. Chemical enhancers (CEs) are a means to enhance drug molecule entry into the skin. To date, over 100 chemicals have been shown to act as CEs for improving flux across skin[6]. Polyglyceryl-3 oleate (POCC) serves as a highly lipophilic permeation enhancer with a high molecular weight (M.W. 726.9Da,  $\log P$  6.21). According to Ruan et al.[7], POCC has demonstrated low dose permeation enhancement without high dose irritation. By perturbing stratum corneum lipids, it promotes drug penetration[8]. There is a lack of research investigating its function in semi-solid formulations. As the efficacy of topically applied drugs at relieving pain and inflammation is dependent on its ability to penetrate skin and permeate to the target tissues[9], different formulation ratios were considered to incorporate POCC into O/W creams to allow the drug to be retained in the skin while reducing the systemic absorption of the drug.

In this study, a stable, easy to apply, safe and effective O/W cream containing 0.05% MF and 10% POCC was innovatively prepared by emulsification. Initially, the oil phase, emulsifier, and chemical enhancer were identified through emulsion stability tests and *in vitro* skin retention experiments. The optimal dosage was then determined using Box-Behnken response surface design, resulting in the optimized formulation. The safety and effectiveness of the prepared creams were evaluated by comparing and validating them with the 0.1% MF cream (trade name Elocon®) developed by Merck Sharp & Dohme. This was done through experiments on appearance properties, rheology, *in vivo* tissue distribution and pharmacodynamics. Furthermore, the impact of incorporating POCC on the cohesive energy density in the cream's oil phase was investigated through *in vitro* release study, rheology, and molecular modeling. The effect of POCC incorporation on the skin compatibility of mometasone furoate was studied through tape stripping, confocal laser scanning microscopy (CLSM), attenuated total reflection Fourier-transform infrared spectroscopy (ATR-FTIR) and small-angle X-ray scattering (SAXS). These findings provide valuable insights for the development of semi-solid formulations.

## 2. Materials and methods

### 2.1. Materials and animals

Mometasone furoate (MF), Isopropyl palmitate (IPP), Isopropyl myristate (IPM), 2,4-dinitrofluorobenzene (DNFB) were purchased from Shanghai Macklin Biochemical Co., Ltd. (Shanghai, China). N-methyl-2-pyrrolidone (NMP), Oleinic acid (OA) was purchased from Alfa Aesar (MA, USA). Maisine® CC, Labrafac™ lipophile WL 1349(LWL1349), Gelot™ 64, Labrafil®M1944CS (LM1944), Plurol®Oleique CC 497 (Polyglyceryl-3 oleate, POCC), Transcutol®P (TP), Lauroglycol®FCC (FCC) were purchased from GATTEFOSSé (Shanghai, China); HPLC grade methanol was purchased from Tianjin Concord technology

Co., Ltd. (Tianjin, China); All of the reagents used in the cream were of reagent grade and obtained commercially. The structures of the MF and permeation enhancers in formulation are shown in Fig. 1.

Wistar rats (male,  $200 \pm 20$  g), mice (male,  $20 \pm 2.0$  g) and Japanese white rabbits (male,  $2.0 \pm 0.5$  kg) were provided by the Experimental Animal Center of Shenyang Pharmaceutical University (Shenyang, China). All animal experiments were conducted in accordance with NIH Guidelines to Care and Use of Laboratory Animals and the Guide to animal use published by the Life Science Research Center of Shenyang Pharmaceutical University (SYPUIACUC-C2021-6-1-18).

## 2.2. Formulation optimization

### 2.2.1. Preparation of creams

The main components of the O/W cream are the oil phase, the water phase and the emulsifier. Screening of four oil phases (Maisine® CC, LWL 1349, IPP, and Cetyl alcohol) and emulsifier (Tween 80, Span 60, Gelot® 64, LM1944). The amount of emulsifier in the formulations was determined based on the hydrophilic-lipophilic balance (HLB) values, as shown in Eq. (1), where A% and B% represented the weight ratio (w/w) of the emulsifier and co-emulsifier.

$$HLB = HLB_A \times A\% + HLB_B \times B\% \quad (1)$$

The cream was prepared using the emulsification method, following these steps: 0.05% (w/w) of MF was dissolved in NMP (The saturated solubility of MF in NMP is 6.76 mg/mL), then oil phase and emulsifier were added to the dissolved drug, melted at 75°C and stirred well. The aqueous phase included deionized water and propylene glycol mixed uniformly at 75°C. The aqueous phase was added to the oil phase of the same temperature by mixing for 5 min at 500 rpm with magnetic stirring (CJJ-6, Shanghai, China) until the primary cream was formed. Upon emulsification, the system was continued to be stirred at 500 rpm until it reached room temperature.

### 2.2.2. Stability study

The creams underwent a stability test to ensure their quality. Centrifugal stability experiments were performed to detect whether phase separation occurred in the cream by centrifuging 1 g of cream at 25°C for 30 min at 5000 r/min on 1 day, 7 days, 14 days, 21 days and 28 days after the preparation of the cream. Meanwhile, the prepared creams were placed at  $8^\circ\text{C} \pm 2^\circ\text{C}$ ,  $25^\circ\text{C} \pm 2^\circ\text{C}$  and  $40^\circ\text{C} \pm 2^\circ\text{C}$  and the appearance of the creams and phase separation were observed at the same time intervals as in centrifugal experiments[10].

### 2.2.3. *In vitro* skin permeation/retention study

To compare the effects of different chemical enhancers on the transdermal absorption of MF in creams, *in vitro* skin permeation/retention experiments were conducted. Male rats were anesthetized with urethane (20%, w/v) and the abdominal hair was carefully shaved off using clippers and electric shavers. The entire skin from the shaved area was excised and the subcutaneous adipose tissue was removed.

Microscopic examination was performed to ensure that the skin was undamaged[11]. The excised skin samples were stored at -70°C and utilized within a month.

The *in vitro* drug skin administration study involved skin retention and permeation studies to observe skin absorption behaviors of the drug. The experiments were conducted using Franz diffusion cells at a temperature of 32°C. The diffusion cells consisted of a donor cell and a receptor cell and were placed in an upright transdermal diffusion system. A cream formulation weighing 250 mg (containing 0.125 mg or 0.250 mg of MF) was applied to the skin, and 15% PEG 400 (4 ml) was used as the receptor fluid to maintain a sink condition. After 8 hours 1.0 ml of receptor fluid was withdrawn for analysis. At the end of the drug skin permeation/retention study, the skin was removed from the diffusion cell to collect the retained drug. The residual cream on the skin was wiped off using a water-moistened cotton swab (recovery rate > 98%). The skin diffusion area was then excised, immersed in methanol and sonicated for 30 minutes. After centrifugation for 5 minutes at 16,000 rpm, the drug content was determined using high-performance liquid chromatography (HPLC) with a C18 column (200 mm × 4.6 mm, 5µm) for sample separation. The flow rate was set at 1.0 ml/min, and the column temperature was maintained at 40°C. The mobile phase consisted of a mixture of methanol and distilled water in a ratio of 80:20.

## **2.2.4. Box-Behnken Design determines optimized formulation**

The Box-Behnken Design (BBD) response surface methodology is an optimization method capable of integrated experimental design and mathematical modeling with good predictability[12]. After determining the types of excipients through stability study, Design Expert software V13.0.1.0 was employed to select the key influencing factors: IPP, POCC and PG, and determine their respective dosages. The experimental design was based on the BBD, which incorporates three levels of experiments. The dosage ranges for the three excipients are presented in Table 1. The response variable chosen for this study was the skin retention (Y) of the creams. The BBD consisted of 17 experimental runs, allowing us to develop a mathematical model that established the relationship between the independent variables (IPP, POCC, PG) and the response variable (skin retention). Through the fitting model, the formula with the highest predicted skin retention was determined. This formula was subsequently verified through the "*in vitro* skin permeation/retention study" to confirm the optimized formulation.

Table 1  
Variables and Levels in the Box-Behnken Design

Independent variables	Levels		
	Units	Low	High
IPP-A	%	3	5
POCC-B	%	5	10
PG-C	%	2	5
Dependent variables	Low	High	Objective
Skin retention-Y	0	100	Maximize

## 2.3. Formulation evaluation

### 2.3.1. Macro and micro structure

The creams were subjected to macroscopic observation to assess their overall appearance. Additionally, microscopic observation was performed using optical microscopy (XSP-2CA, Shanghai). To facilitate the examination, the samples were appropriately diluted. To simulate the actual conditions during the *in vitro* permeation/retention study, the creams used in this particular section were aged for 24 h prior to examination.

### 2.3.2. Particle size measurement

Approximately 1 g of the cream was added to 100 ml of water for pre-dispersion. Using a Malvern Laser Particle Size Analyzer (Mastersizer 2000MU), the pre-dispersed sample was added to the cuvette with a shade of approximately 10%-15% and the test was averaged over three times.

### 2.3.3. Rheology

A rheological investigation was conducted to characterize the cream's fluidity using an AR 2000 rheometer from TA Instruments (USA). A 0.5 g sample of the MF cream was applied to a parallel-plate geometry with a diameter of 20 mm. Prior to the rheological analysis, a 2-minute equilibration period was employed to eliminate potential factors that could influence the test results[13].

Oscillation strain sweep: The cream was subjected to varying shear strain ranging from 0.01–100% at a frequency of 1 rad/s to identify its linear viscoelastic region (LVR). The values of the storage modulus ( $G'$ ) and loss modulus ( $G''$ ) were then utilized to assess the cream's viscoelastic properties.

The steady flow behavior: In order to examine the flow characteristics of the different creams under controlled shear conditions, a shear rate range of 0.01–100  $s^{-1}$  was selected and all samples were subjected to this specific test condition for data acquisition.

Thixotropy test: The shear rate is systematically increased from 0 to  $20 \text{ s}^{-1}$  and subsequently decreased back to 0, allowing for the measurement of shear stress changes corresponding to the rate. These measurements generate a closed curve referred to as the thixotropic loop or thixotropic ring. This curve can be served as an indicator of the cream's thixotropic behavior.

### **2.3.4 Skin irritation experiment**

The skin irritation experiment was performed on the abdomen of male rabbits[14]. The abdominal hair of the rabbits was shaved 12 h prior to dosing to ensure the integrity of the skin. Four groups were designed: the basic formulation group, the optimized formulation group, acutely broken skin group (sandpapered the skin and applied the optimized formulation after bleeding spots appeared) and positive control group (0.5 ml of 10% SDS applied for 8 h). 0.5g of cream was taken and applied to the skin, covered with gauze and fixed with tape. Photographs were taken 1h and 8h after administration and 0h, 24h and 48h after wiping with warm water.

### **2.4. *In vivo* tissue distribution study**

The *in vivo* tissue distribution experiment was conducted to validate the findings from the *in vitro* experiment. The abdominal hair of male Kunming mice ( $20 \text{ g} \pm 2 \text{ g}$ ) was removed 24 h in advance, provided by the Experimental Animal Center of Shenyang Pharmaceutical University. The cream (250mg) was applied to the skin with an area of  $1.77 \text{ cm}^2$  and blood samples (0.5ml) were collected at 1, 2, 3, 5, 8, 12, 16, 24, 32, 48 h[15], that the remaining creams were wiped clean at 8 h. After the designated time points, the mice were euthanized, and the skin and muscle at the administration site were collected. The detection method of drug concentration in tissue was consistent with that in the *in vitro* test. And the plasma was treated as follows: the samples were centrifuged at 16,000 rpm for 5 min at  $15^\circ\text{C}$ . Then, internal standard (clascoterone, 100ng/ml,  $10\mu\text{l}$ ) and plasma ( $100\mu\text{l}$ ) were eddied for 20 s. The extractant ethyl acetate (1ml) was added to the mixture and mixed for 3 min, then centrifuged for 5 min at  $-5^\circ\text{C}$ , 16,000 rpm. The extraction solution was subsequently evaporated by nitrogen stream at  $40 \pm 1^\circ\text{C}$  to dry. Finally, the mobile phase was added ( $200\mu\text{l}$ ) to dissolve, eddied for 3 min, centrifuged at  $-5^\circ\text{C}$  for 5 min and took supernatant to determine drug concentration. The supernatant was collected for LC-MS/MS analysis, which consisted of an Agilent 1290 Infinity II UHPLC system (Agilent Technology, Santa Clara, CA, USA) equipped with an AB Sciex API TRIPLE QUADTM 4500 mass spectrometer (Sciex, Framingham, MA, USA). For chromatography, a reversed-phase column (Waters Poroshell UPLC EC C18,  $1.9\mu\text{m}$ ,  $2.1 \times 50 \text{ mm}$ ) was used. The mobile phase was methanol: water (0.3% formic acid) = 80: 20 (v/v) with a flow rate of 0.3 ml/min. The column temperature was kept at  $30^\circ\text{C}$ .

### **2.5. Establishment of chronic atopic dermatitis model in mice**

A mouse model of chronic atopic dermatitis was established through DNFB-induced sensitization to assess the effectiveness of the formulation[16]. To establish the model, the abdominal region of the mice was shaved 24 hours prior to the experiment. On the first day,  $100\mu\text{l}$  of a 7% DNFB acetone-olive oil

solution was applied to the abdomen for sensitization. Subsequently, on the 5 8 11 and 14 days of the experiment, 20 $\mu$ l of a 0.5% DNFB solution was uniformly applied multiple times to the inner and outer surfaces of the right ear to induce excitation. The control group received an application of acetone-olive oil solution (4:1) on the abdomen and ears. Drug treatment commenced 24 hours after the final excitation, with the positive control group not receiving any treatment. The treatment groups included the Elocon® cream group, the basic formulation group and the optimized formulation group ( $n = 6$ ). Each group received a daily application of 0.1 g of the respective cream, with the inner and outer surfaces of the right ear being gently rubbed using a glass rod for approximately 5s until the 3rd day after the final excitation. At the conclusion of the experiment, the mice were euthanized, and the middle section of the right and left ears were obtained using a 6 mm punch. The weight difference between the two ears was measured and the right ear was collected for histopathological examination after hematoxylin and eosin (H&E) staining.

## 2.6. Enhancement action mechanism characterization

To be effective, the drug contained in the cream must first be released from the matrix and then penetrate the skin to exert its pharmacological effect. This study comprehensively investigated the molecular mechanisms underlying the incorporation of POCC for the release of MF and its retention in the skin, through the application of *in vitro* release study, rheology, molecular modeling, tape stripping study, CLSM, ATR-FTIR, SAXS and molecular docking characterization.

### 2.6.1. *In vitro* release study

To investigate the impact of POCC addition on the drug release behavior of MF, drug release experiments were carried out through the diffusion cell mentioned previously. Instead of using skin, a semipermeable membrane known as Cellophane® was employed as a substitute. The 0.25g cream was applied onto the Cellophane® membrane, and samples (1.0ml) were collected at specific time points (0.5, 1, 2, 4, 6, 8 h). To maintain a sink condition, an equal volume of fresh 30% ethanol was immediately added to the cells after each collection[17]. The determination of drug concentration in the collected samples followed the same protocol as the "*In vitro* skin permeation/retention study."

### 2.6.2. Molecular modeling

The molecular modeling study was conducted using Materials Studio software (version 7.0, Accelrys Inc., San Diego, CA, USA) to obtain molecular-level insights into the interactions between MF, POCC and IPP, as well as their correlation with the rheological properties of the creams. Firstly, all structures were geometrically optimized by Forcite module. Molecular docking was then performed in Blends module and atom-based geometric optimization was performed using COMPASS II force field. According to the principle of molecular dynamics, the cube box simulation system of drug and PSA was constructed by using Amorphous Cell module according to the optimized formula ratio[18].

Subsequently, the 30ps NVT balance was performed for each system. Then the 300ps molecular dynamics simulations of various systems in NPT were carried out at 305k and 101kPa, and the



equilibrium structures were obtained. Finally, cohesive energy density (CED) and mean square displacement (MSD) were obtained. And diffusion coefficient ( $D'$ ) was calculated by Eq. (2), the Einstein's Eq.:

$$D' = \frac{1}{2t} \lim_{t \rightarrow \infty} \langle [z(t) - z(0)]^2 \rangle$$

2

Where  $t$  is time, and  $z(0)$  and  $z(t)$  are the  $z$  components of the particle positions at times 0 ps and  $t$  ps, respectively.  $D'$  was one-sixth of the slope of MSD -  $t$  curve in molecular dynamics simulations.

### 2.6.3. Tape stripping study

The tape stripping test was employed to investigate the distribution of MF within the stratum corneum (SC), viable epidermis and dermis (VE&DE). After an 8 h *in vitro* permeation/retention experiment, the skin was subjected to 10 consecutive tape stripping procedures using adhesive tapes to collect the retained amounts of MF in the SC and VE&DE layers, respectively[19]. The analysis of MF was conducted following the same method as the "*In vitro* skin permeation/retention study."

### 2.6.4. CLSM

CLSM was utilized to visualize the skin enhancement effect of POCC. The fluorescent probe FITC was used in this study. FITC shares structural similarities with MF, possessing carbonyl groups at the C3 position, and serves as the pharmacodynamic group of MF[4]. The FITC and POCC were added into ethanol, sonicated for 30 mins then centrifuged and the supernatants were used as donor solutions. FITC in ethanol without POCC was used as a control group. The obtained solution was added to the skin for 1 h. Afterward, the skin was washed with distilled water and dried with filter paper to remove the excess solution on its surface. The skin sample was directly sandwiched between a coverslip and a glass slide. CLSM analysis was performed with a LSM 710 Laser Scan Microscope (Carl Zeiss AG, Jena, Germany). FITC was excited at 488nm wavelength using an argon laser (FITC excitation 495nm, emission 521nm) [20]. Depth scans were conducted at 5 $\mu$ m intervals, reaching a maximum depth of 30 $\mu$ m.

### 2.6.5. ATR-FTIR spectra

ATR-FTIR was conducted to examine the lateral organization and conformational ordering of skin lipids[21]. Four samples were studied: i) ethanol (EtOH); ii) EtOH with 0.05% MF; iii) EtOH with 10% POCC; iv) EtOH with 0.05% MF and 10% POCC. The control group consisted of skin treated with EtOH alone. The samples were added to the skin and left for 8h. Then, the skin surface was wiped with cotton. The whole skin and the VE&DE layer remaining after tape stripping were placed facing zinc selenide (ZnSe) crystals. The ATR-FTIR spectra were collected from instruments (Bruker, Ettlingrn, Germany) equipped with an ATR tool and MCT detectors in the frequency range of 4000 - 700  $\text{cm}^{-1}$ .

### 2.6.6. Small-angle X-ray scattering (SAXS) spectra

Small-angle X-ray scattering (SAXS) was employed to investigate the structural changes in skin components, including lipids and proteins. SC samples were treated with a pH 7.4 phosphate buffer solution containing 10% (w/v) trypsin at 37°C. After 24h, each layer of skin was separated with tweezers, the SC layer was washed with deionized water, and the separated skin tissue was wiped with cotton before vacuum drying. Before the experiment, the SC layer was soaked in i) EtOH and ii) EtOH with 10% POCC solutions at room temperature for 8h, and then, the solvent was dried to obtain skin samples. The X-ray diffraction used an imaging plate system (R-Axis IV; Anton Pal, Austria), and the beam was the BL40B2 (Structural Biology II BeamLine) of Spring-8 (Anton Paar, Austria). The X-ray imaging plate area was 30 mm × 30 mm, the wavelength was 0.0709 nm, and the exposure time was 900 s. The reciprocal spacing ( $S = (2/\lambda) \times \sin \theta$ ) was calibrated from the lattice spacing of silver benzoate at room temperature ( $d = 5.838$  nm, where  $d$  is the layered repetition distance), where  $2\theta$  is the scattering Angle [22]. Photon counting was performed at 1152 pixels in the range of  $S = 0.05\text{--}0.2$  nm<sup>-1</sup> to determine the number of photons at each pixel.

## 2.6.7. Molecular docking

Molecular interactions between MF, POCC and skin/body fluids were studied by molecular docking. The collagen (COL) molecule was used as a model for the viable epidermis and dermis (VE&DE), while water (H<sub>2</sub>O) represented the body fluids. Key molecular parameters, such as the interaction parameter ( $\chi$ ) and the mixing energy ( $E_{\text{mix}}$ ), were calculated to provide insights into the MF-POCC-skin/body fluids interactions at a molecular level.

## 3. Results

### 3.1. Formulation optimization

#### 3.1.1. Stability study

The types of excipients and the composition of the formulations are shown in Table 2. The stability of the five creams that were prepared has been evaluated and the findings were depicted in Fig. 2a. F1 precipitated out of the oil phase after 28 days of storage. F2 precipitated out of the oil phase after 7 days of storage at  $40 \pm 2^\circ\text{C}$ . F3 was centrifuged after 7 days of storage. F4 was centrifuged after 14 days of storage. F5 was stable under all conditions, and therefore, the oil phase of the formulation was selected to be an IPP, with an emulsifier of Gelot® 64 and a co-emulsifier of LM1944.

Table 2  
Composition of the formula and the proportion of components

Ingredients		Formulations				
		F1 (%)	F2 (%)	F3(%)	F4 (%)	F5 (%)
API	MF	0.05	0.05	0.05	0.05	0.05
Solubilizer	NMP	1	1	1	1	1
Oil phase	Maisine® CC	20	-	-	-	-
	LWL1349	-	20	-	-	-
	IPP	-	-	5	5	5
	Cetyl alcohol	5	5	6	4	4
Emulsifiers	Tween 80	4	4	4	2	-
	Span 60	-	-	-	4.2	-
	LM1944	-	-	-	-	2
	Gelot® 64	-	-	-	-	8
Aqueous phase	PG	5	5	5	5	5
	Water	To 100g				

### 3.1.2. The effect of chemical enhancers

After determining the type of oil phase and emulsifier by stability studies, the effect of five chemical enhancers: POCC, IPM, FCC, TP and OA (structures shown in Fig. 1) on the retention of MF in the skin was investigated. Using F5 as the basic formulation, the enhancers were added at 10% and the amount of water in the formulation was reduced accordingly. All five formulations containing 10% enhancers passed the stability studies and were subjected to *in vitro* permeation/retention experiment. Since the 8 h cumulative permeation could not reach the limit of quantification by HPLC, only the 8 h cumulative skin retention was measured and compared. The results are shown in Fig. 2b, which demonstrated that POCC achieved the maximum enhancement effect, with a cumulative retention 1.83 times that of the F5 (Table 2) ( $p < 0.05$ ). Thus, POCC was chosen as the skin retention enhancer for the MF cream.

### 3.1.3. Box-Behnken Design determines optimized formulation

The BBD was employed to optimize the dosage of the three influential factors. The performance of the cream was influenced by various factors that did not act independently, as they had interdependencies and mutual effects on each other. The nonlinear fitting models (Skin retention =  $5.12 - 0.2147 \times \text{IPP} + 1.270 \times \text{POCC} - 1.260 \times \text{PG} - 0.0630 \times \text{IPP} \times \text{POCC} + 0.5280 \times \text{IPP} \times \text{PG} - 0.5955 \times \text{POCC} \times \text{PG} - 0.8961 \times \text{IPP}^2 -$

$0.6101 \times \text{POCC}^2 - 0.9111 \times \text{PG}^2$ ,  $R^2 = 0.8552$ ,  $P < 0.0020$ ) were conducted to predict the dosage of the three factors and the relationship between the combined response value (skin retention and stability), and the influencing factors were reflected in the 2D&3D surface map in Fig. 2c-d directly [23]. Based on the response surface analysis, the optimized formulation excipients and their concentrations were shown in Table 3. The predicted optimized formulation was validated against F5 (basic formulation) and Elocon® cream in *in vitro* skin permeation/retention study and the results in Fig. 2e showed that the retention of the optimized formulation ( $7.71 \mu\text{g/g}$ ) was increased by 2.48-fold as compared to the basic formulation ( $3.10 \mu\text{g/g}$ ), and there was no significant difference in retention with Elocon® cream ( $6.79 \mu\text{g/g}$ ).

Table 3  
Composition of the optimized formulation for  
BBD prediction

Ingredients	Optimized formulation F6 (%)
MF	0.05
NMP	1
IPP	4
Cetyl alcohol	4
Gelot®64	8
LM1944	2
POCC	10
PG	2
H <sub>2</sub> O	Add to 100

## 3.2. Formulation evaluation

### 3.2.1. Macro and micro structure

According to the observation in Fig. 3a, the optimized formulation appeared as a white cream with a glossy texture. Microscopic examination revealed that the cream exhibited evenly distributed droplets with uniform particle sizes. This observation suggested that the inclusion of POCC in the formulation significantly improved the cream's appearance and microstructure.

### 3.2.2 Particle size measurement

The particle sizes as shown in Fig. 3b. In the basic formulation, D10 D50 and D90 were  $3.93 \mu\text{m}$ ,  $4.50 \mu\text{m}$  and  $5.06 \mu\text{m}$ , PDI was 0.321. In the optimized formulation, the particle sizes were  $6.06 \mu\text{m}$ ,  $6.81 \mu\text{m}$  and  $7.67 \mu\text{m}$ , PDI was 0.125. The results indicated that the incorporation of POCC resulted in an augmentation of the emulsion droplet size and a uniform particle size distribution, as observed by microscopy.

### 3.2.3. Rheology

#### Oscillation strain sweep

From the obtained Fig. 4a, which depicts the  $G'$  and  $G''$  values plotted against the strain, it is evident that both the creams exhibit a predominant elastic behavior within the linear viscoelastic region (LVR), as the  $G'$  value is greater than the  $G''$ . The corresponding rheological oscillatory parameters for the strain sweep, including the  $G'$ ,  $G''$  and  $\tan \delta$  are summarized in Table 4. It can be observed that the optimized cream demonstrates lower values for these parameters, indicating that it is softer. [13].

Table 4  
Rheological data obtained from the oscillation strain sweep test for the three creams ( $n = 3$ ).

Creams	$G'$ (Pa)	$G''$ (Pa)	$\tan \delta$
Basic	4602	3536	0.77
Optimized	1685	1412	0.84

#### The steady flow behavior

Figure 4b illustrates that both the creams exhibit non-Newtonian fluid behavior. Based on the experimentally observed data, suitable mathematical models such as the Power-Law (PL) relation and Herschel-Bulkley (HB) model were employed to effectively fit the relevant factors[24]. These models are mathematically stated by Eq. (3) and Eq. (4),

$$\text{PL-based model: } \tau = K\gamma^n \quad (3)$$

$$\text{HB-based model: } \tau = \tau_0 + K\gamma^n \quad (4)$$

where  $\tau$  denotes the shear stress,  $\tau_0$  is the yielding stress,  $K$  represents the consistency coefficient,  $\dot{\gamma}$  denotes the shear rate of unit 1/s, and  $n$  represents the index of the flow behavior.

The fitting results shown in Table 5 indicate that the basic and optimized formulations fit the Herschel-Bulkley model better and both exhibit plastic fluid behavior. The optimized formulation displays a lower  $\tau_0$ , indicating lower viscosity and yield stress compared to the basic formulation group. The inclusion of POCC enhances the fluidity of the formulation, facilitating easier spreading of the cream.

Table 5  
Parameters fitted by the PL and HB models for the behavior of the steady flow ( $n = 3$ ).

Creams	PL-based model		HB-based model		
	R <sup>2c</sup>	K (P· s <sup>n-1</sup> )	R <sup>2</sup>	$\tau_0$ (pa)	K (P· s <sup>n-1</sup> )
Basic	0.9530	127.7	0.9557	12.83	115.55
Optimized	0.9340	115.0	0.9350	8.012	104.9

c R<sup>2</sup> stands for the correlation coefficient.

### Thixotropy test

The results depicted in Fig. 4c reveal that the optimized formulation exhibited a complete thixotropic ring, indicating significant thixotropic properties. In contrast, the basic formulation demonstrates relatively lower thixotropic characteristics. The incorporation of POCC enhanced the thixotropic properties of the cream and facilitated the diffusion and absorption of the drug within the skin [25].

## 3.2.4. Skin irritation experiment

The results of the cream irritation experiment are shown in Fig. 4d. In the positive control group, SDS produced strong irritation to the skin, making the skin red and swollen and peeling. The optimized formulation was not significantly irritating to both normal rabbit skin and acutely broken skin. The results showed that all of the MF creams weren't significantly irritating to rabbit skin.

## 3.3. *In vivo* tissue distribution study

Figure 5 illustrates the concentrations of the drug in the skin, muscle and plasma at different time points following the topical administration of MF cream in mice. The cumulative concentration in the skin gradually increased with the duration of administration, peaking at  $2.67 \pm 0.27 \mu\text{g/g}$  after 16 h in the optimized formulation, and subsequently exhibited a declining trend. In contrast, the maximum concentrations in muscle and plasma were only  $0.19 \pm 0.02 \mu\text{g/g}$  and  $126 \pm 11.59 \text{ ng/ml}$ , respectively. The amount of the optimized formulation in the skin, muscle and plasma *in vivo* was more than two times that of the basic formulation, consistent with the results of the *in vitro* experiments. And there was no significant difference between the optimized formulation and Elocon® cream. These results indicated that POCC played a significant role in promoting the entry of MF from the cream into the skin.

## 3.4. Pharmacodynamics

Following the administration of 0.1% DNFB stimulation, mice exhibited erythema and scratching behavior in their ears after 1 h. Figure 6a demonstrates the final weight differences in the ears of the mice, with the optimized formulation showing the most significant reduction of 59.52% ( $*P < 0.05$ ) compared to the

positive control group. The Elocon® cream exhibited a reduction of 52.80% (\* $P < 0.05$ ) and the basic formulation showed a reduction of only 12.70%. Moreover, a significant difference was observed in the weight difference between the optimized formulation and the basic formulation (# $P < 0.05$ ). Representative photographs of mouse ears and the results of H&E-stained pathological sections are presented in Fig. 6b. The normal mouse ear skin exhibited a clear structure with normal epidermal thickness, no signs of edema, and no lymphocyte infiltration. In contrast, the positive control group and the basic formulation displayed hyperkeratotic epidermis, thickening, scabs and significant infiltration of mixed inflammatory cells in the dermis, such as lymphocytes and histiocytes. The capillaries were dilated and congested. Treatment with the Elocon® cream and the optimized formulation resulted in reduced epidermal thickening, alleviation of epidermal and dermal edema, reduced lymphocyte infiltration and mitigation of dermal vasodilation and congestion. These results demonstrated that the addition of POCC enabled the MF cream to exhibit a favorable anti-inflammatory effect.

## 3.5. Enhancement action mechanism characterization

### 3.5.1. *In vitro* release study

As depicted in Fig. 7a, the *in vitro* drug release profiles demonstrate that the cumulative release of MF at 8 h was 1.77 times greater in the optimized formulation containing 10% POCC compared to the basic formulation ( $P < 0.05$ ). The results suggest that POCC plays an important role in the release of the drug from the cream.

### 3.5.2. Rheology

The data of "Oscillation strain sweep" were also used to obtain the parameter critical strain  $\gamma_c$  (the value when  $G'$  decreases to 95% of its initial value) and cohesive energy density ( $E_c$ ), which was calculated from Eq. 5[26]:

$$E_c = \frac{1}{2} G' \gamma_c^2$$

5

The results presented in Table 6 indicate that the inclusion of POCC reduced the cohesive energy density of the cream's oil phase from  $4.988 \times 10^{-4} \text{ J/m}^3$  to  $2.233 \times 10^{-4} \text{ J/m}^3$ . This decrease in cohesive energy density enhanced the fluidity and flowability of the cream. Furthermore, it improved the thermodynamic activity of MF within the cream, facilitating the release of MF from the cream matrix.

Table 6  
The storage modulus  $G'$ , the critical strain  $\gamma_c$  and the  $E_c$  of the basic and optimized formulations determined by rheology

	$G'$ (Pa)	$\gamma_c$ (%)	$E_c$ (J/m <sup>3</sup> )
Basic	763.1	0.0362	$4.988 \times 10^{-4}$
Optimized	340.2	0.0362	$2.233 \times 10^{-4}$

### 3.5.3. Molecular modeling

Molecular simulations were used to validate the rheological results and to further investigate the interaction of MF, POCC and IPP. From Fig. 7b-d, it can be seen that there is no hydrogen bonding interaction between IPP and MF; hydrogen bonding is formed between POCC and IPP with a distance of 2.704Å, and this hydrogen bonding disappears when MF and POCC are docked to IPP at the same time, but hydrogen bonding with a distance of 2.917Å is formed between POCC and MF, suggesting that there is a strong interaction between POCC and MF.

Through kinetic simulations, two crucial parameters were calculated for MF and MF-POCC in the oil phase (Fig. 7e-g): the diffusion coefficient ( $D'$ ) and the cohesive energy density (CED). The former indicates the mobility of the drug in the cream, the higher the value the greater the mobility; the latter is used to measure the interaction between the drug and the cream, the higher the value the stronger the interaction[27]. The  $D'$  values for MF and MF-POCC were determined as  $7.69 \times 10^{-13}$  m<sup>2</sup>/s and  $1.27 \times 10^{-12}$  m<sup>2</sup>/s, while the CED values were found to be  $3.78 \times 10^8$  J/m<sup>3</sup> and  $3.21 \times 10^8$  J/m<sup>3</sup>, respectively. The molecular modeling results revealed that the addition of POCC to the cream enhanced the drug's diffusion behavior and weakened the interaction between the drug and the oil phase of the cream. Consequently, this improvement contributed to the enhanced release of the drug from the cream.

### 3.5.4. Tape stripping study

The tape stripping study was used to clarify the enhancement effect of POCC on skin retention. As shown in Fig. 8, after 8 hours of *in vitro* skin penetration, MF in the optimized formulation was mainly retained in the viable epidermis and dermis (VE&DE); however, in the basic formulation, MF was mainly retained in the stratum corneum (SC), indicating that the addition of POCC enhanced MF penetration into deeper skin layers.

### 3.5.5. CLSM

To visualize the skin penetration process of the drug, confocal laser scanning microscopy (CLSM) was employed. Figure 9 presents the CLSM images depicting the skin penetration of FITC. On the skin surface, a brick mortar structure comprising flat hexagonal keratinocyte structures was observed, suggesting that FITC penetrated the skin through the intercellular lipid pathway. In the control group, FITC was detected



up to a depth of 10 $\mu$ m. However, when 10% POCC was incorporated, the penetration of the FITC probe increased to a depth of 25 $\mu$ m. This observation confirms that the addition of POCC facilitated the entry of the MF into VE&DE layers of the skin, consistent with the findings from the *in vitro* skin distribution study.

### 3.5.6. ATR-FTIR spectra

The characteristic peaks of the skin were observed using ATR-FTIR to investigate the effect of POCC on the skin. As shown in the Fig. 10a, the addition of 10% POCC caused a red shift in the symmetric ( $\nu$ sCH<sub>2</sub>, 2850 cm<sup>-1</sup>) and asymmetric ( $\nu$ asCH<sub>2</sub>, 2920 cm<sup>-1</sup>) stretching vibration peaks of SC lipids, which was further enhanced when POCC and MF were mixed. However, POCC had no significant effect on the amide II band (1541 cm<sup>-1</sup>) and the amide I band (1646 cm<sup>-1</sup>) of SC keratin. In the hydrophilic region below the SC, including the viable epidermis and dermis (Fig. 10b), POCC affects the  $\nu$  C-O-C (1081 cm<sup>-1</sup>) of collagen (COL) and  $\nu$ asPO<sup>2-</sup> (1237 cm<sup>-1</sup>) stretching of phospholipids in VE&DE when added to the skin in mixture with MF[28]. It could be seen that the addition of POCC disorganized the arrangement of lipids in the SC of the skin and promoted the entry of MF, and when both POCC and MF were present, they formed hydrogen bonds with collagen in the VE&DE layer, which was retained in the skin.

Small-angle X-ray diffraction profiles of SC. (d) The Repeat Distance of SC Obtained from the 2nd-Order Diffraction Peak for the Long Lamellar Structure and the 1st-Order Diffraction Peak for the Short Lamellar Structure. Minimum energy complexes of (e) POCC-MF with COL, (f) POCC-MF with H<sub>2</sub>O.

### 3.5.7. Small-angle X-ray scattering spectra

The small-angle X-ray scattering was used to characterize the structure of the intercellular lipids at the molecular level to determine the barrier function of the SC layer. The stratum corneum (SC) contains intercellular lipids that are organized in lamellar structures with specific repeat distances. These structures are known as the long-periodicity phase (LPP) and short-periodicity phase (SPP), with lengths of 13 nm and 6 nm, respectively. Figure 10c-d presents the repeat distances of these lamellar structures in the SC following treatment with MF and POCC ethanol solutions. The addition of 10% POCC ethanol solution decreased the LPP from 13.69 nm to 13.11 nm, but it had no effect on the SPP (both 6.024 nm). This finding, combined with the ATR-FTIR results, suggests that POCC disrupts the LPP structure of skin lipids, thereby allowing MF to enter the skin.

### 3.5.8. Molecular docking

The interaction of POCC with MF and skin/body fluids was explored by molecular docking. The results, as shown in Fig. 10e-f, reveal the optimal conformation of POCC-MF with collagen (COL) and water (H<sub>2</sub>O). POCC forms hydrogen bonds with COL and MF, with bond lengths of 2.812 Å and 2.917 Å, respectively. This interaction acts as a bridge connecting the drug to the viable epidermis and dermis (VE&DE) layer through hydrogen bonding.

In general, the lower the values of  $E_{mix}$  and  $\chi$ , the better the compatibility of the two molecules and the more stable the binary system they form. According to the calculations in Table 7, the  $E_{mix}$  and  $\chi$  of the COL-POCC-MF system are lower than those of the H<sub>2</sub>O-POCC-MF system, indicating that POCC-MF is more stable in the VE&DE layer and tends to be retained in the skin.

Table 7  
Interaction parameter ( $\chi$ ) and blending energy ( $E_{mix}$ ) of Collagen (COL), H<sub>2</sub>O, MF and POCC.

	$\chi$	$E_{mix}$
COL-MF	34.44	20.40
COL-POCC	29.33	17.37
COL-POCC-MF	21.22	12.57
H <sub>2</sub> O-MF	34.42	20.38
H <sub>2</sub> O-POCC	39.27	23.25
H <sub>2</sub> O-POCC-MF	37.34	22.11

## 4. Discussions

In the present study, a cream containing 0.05% MF was developed and the enhancing effect of POCC on drug release and skin retention was elucidated at the molecular level. Chemical permeation enhancers are a useful method for enabling drugs to penetrate the skin barrier and have local or systemic effects. POCC possesses high lipophilicity and a high level of safety, resulting in better permeation enhancement effects in patches[29]. The addition of any excipient in semi-solid formulations can impact the stability of the formulation. However, in this study on formulation optimization, the addition of POCC had no impact on the stability of the O/W MF cream, but instead resulted in a cream that was glossier, had a more uniform particle size distribution, and lower viscosity and yield stress. This made the cream easier to apply and improved patient compliance. Skin irritation study also demonstrated the safety of creams containing POCC (Fig. 4).

The efficacy of the drug from the cream to the site of action on the skin is mainly influenced by two aspects, firstly the drug has to be released from the cream and later the skin barrier has to be opened to enter the skin[8]. The addition of different ingredients to the cream has different effects on the size of the cream droplets and the flowability of the cream, and these changes further affect the drug release and skin retention of the drug. the addition of POCC causes a significant decrease in the energy storage modulus of the cream, which is due to the plasticizing effect of POCC on the oil phase[30]. At the molecular level, the plasticising effect leads to an increase in intermolecular space or free volume and may involve the weakening or breaking of selective interpolymer bonds. POCC significantly reduces the

cohesive energy density ( $E_C$ ) of the oil phase, which tends to increase the molecular mobility of the oil phase. In addition, the IPP-POCC-MF system has a higher  $D'$  and lower CED value compared to the IPP-MF system by molecular simulation, which again confirms that the strength of the intermolecular interaction between the oil phase of POCC-MF and cream is weaker than that of MF and cream. The results of rheological experiments (Table 6) and molecular simulations corroborate each other and explain that the increased release of MF from the cream by POCC is due to its reduced interaction with the oil phase of the cream, which increases the fluidity of the cream and accelerates the diffusion of the drug.

In order for a drug to be effective at its target site, the active ingredient in a topical formulation must penetrate the skin barrier, which strictly controls the entry of external substances. This skin barrier consists mainly of the stratum corneum, the outermost layer of the skin, which significantly limits the penetration of drugs. Previous studies have shown that lipophilic permeation promoters are better able to enhance the skin penetration of drugs because they readily mix with the intercellular lipids of the SC, disrupting the lipid arrangement and thus providing better permeability[7]. The molecular mechanism (Fig. 11a) by which the lipophilic permeation promoter POCC enhances drug retention in the skin was investigated using ATR-FTIR spectroscopy and SAXS. The ATR-FTIR results (Fig. 10a) showed that the addition of POCC shifted the spectral band at  $\nu\text{CH}_2$  towards higher wave numbers. This suggests that the site of action of POCC is the alkyl chain of intercellular lipids, and the interaction strength may alter the accumulation of SC intercellular lipids, thereby increasing the distribution of the drug in the skin and facilitating the penetration of MF into the skin[31]. The ATR-FTIR results were further confirmed by SAXS (Fig. 10c-d) that the addition of POCC affected the long period phase of SC lipids and loosened the SC lipid arrangement. The molecular structure of lipids and their arrangement in the lipid layer are considered important for the barrier function of the skin; therefore, POCC disturbed the long-period phase of SC lipids, thus affecting the barrier function of the skin and increasing the entry of MF into the skin.

According to the results of *in vitro* distribution (Fig. 8) and CLSM (Fig. 9) studies, MF was mainly retained in the VE&DE after passing through the SC of the skin, which was consistent with the results of *in vivo* tissue distribution experiments. As shown by the ATR-FTIR (Fig. 10b) results, POCC didn't form hydrogen bonds with the dermis when it was added alone, which was consistent with the results of Xu et al[8]. However, the simultaneous presence of POCC and MF caused the  $\nu\text{C-O-C}$  of collagen and the  $\nu\text{asPO}_2^-$  of phospholipids in the dermis to shift toward the long wavelengths, indicating that there was a hydrogen-bonding interaction between POCC-MF and the dermis (Fig. 11b), which was demonstrated by molecular docking (Fig. 10e-f) It was shown that the incorporation of POCC acted as a bridge, forming hydrogen bonds between the hydroxyl group of POCC and the amide group of the COL, and with the hydrogen bond acceptor Cl of MF. Meanwhile, the  $E_{\text{mix}}$  and  $\chi$  of the COL-POCC-MF system is lower than that of  $\text{H}_2\text{O}$ -POCC-MF (Table 11), indicating that POCC-MF is more compatible with COL and the system they form is more stable, which leads to more retention of MF in the VE&DE rather than penetration into the bloodstream. This allowed the MF to exert higher efficacy while avoiding systemic side effects, proving that the prepared cream was effective and safe.

## 5. Conclusions

In this study, an optimized formulation containing 0.05% MF cream was successfully developed using *in vitro* skin retention studies and BBD. The optimized formulation showed a two-fold improvement in *in vitro* and *in vivo* skin retention compared to the basic formulation, with enhanced pharmacodynamic effects. There was no significant difference compared to commercially available Elocon® cream (containing 0.1% MF). POCC, as a key excipient in the formulation of the cream, decreased the CED of the oil phase of the cream to enhance the drug release, disturbed the long-period phase of the lipids in the SC of the skin and linked the MF to the collagen in the dermis through hydrogen bonding, which increased the retention of the MF in the VE&DE and allowed the drug to exert better therapeutic efficacy. These results provide valuable insights for the development of effective topical formulations in the field of dermatology and beyond.

## Declarations

**Funding** The authors declare that no funding, grants, or other support was received during the preparation of this manuscript.

**Competing interests** The authors declare no competing interests.

### Author information

#### Authors and affiliations

Department of Pharmaceutical Sciences, School of Pharmacy, Shenyang Pharmaceutical University, 103 Wenhua Road, Shenyang 110016, China

Wenxuan Jia Yu Pang Chenyu Zhao Yang Zhang Chao Liu Liang Fang

Key Laboratory of Natural Medicines of the Changbai Mountain, Ministry of Education, College of Pharmacy, Yanbian University, 977 Gongyuan Road, Yanji 133002, China

Yu Cai Liang Fang

**Author contribution** Wenxuan Jia: methodology, investigation, formal analysis, data curation, writing original draft. Yu Pang: Conceptualization, Formal analysis, Writing – review & editing. Chenyu Zhao: Resources. Yu Cai: Writing – review & editing. Yang Zhang: Review & editing. Chao Liu: Project administration. Liang Fang: Conceptualization, Resources, Supervision, Funding acquisition.

**Corresponding author** Correspondence to Liang Fang.

**Availability of data and materials** Data sharing not applicable to this article as no datasets were generated or analyzed during the current study.

**Ethics approval and consent to participate** All animal procedures were approved by the Animal Ethics Committee of Shenyang Pharmaceutical University (approval number: SYPUIACUC-C2021-6-1-18). All animal procedures conformed to the NIH Guide for Care and Use of Laboratory Animals.

**Consent for participate** Not applicable. No human studies have been performed in this research.

**Consent for publication** Not applicable.

## References

1. Langan SM, Irvine AD, Weidinger S. Atopic dermatitis. *The Lancet*. 2020;396(10247):345–60. [https://doi.org/10.1016/s0140-6736\(20\)31286-1](https://doi.org/10.1016/s0140-6736(20)31286-1).
2. Weidinger S, Baurecht H, Schmitt J. A 5-year randomized trial on the safety and efficacy of pimecrolimus in atopic dermatitis: a critical appraisal. *Br J Dermatol*. 2017;177(4):999–1003. <https://doi.org/10.1111/bjd.15827>.
3. Abuabara K, Hoffstad O, Troxel AB, Gelfand JM, McCulloch CE, Margolis DJ. Patterns and predictors of atopic dermatitis disease control past childhood: An observational cohort study. *J Allergy Clin Immunol*. 2018;141(2):778–780e6. <https://doi.org/https://doi.org/10.1016/j.jaci.2017.05.031>.
4. Mehta A, Nadkarni N, Patil S, Godse K, Gautam M, Agarwal S. Topical corticosteroids in dermatology. *Indian J Dermatology Venereol Leprology*. 2016;82(4). <https://doi.org/10.4103/0378-6323.178903>.
5. Spada F, Barnes TM, Greive KA. Comparative safety and efficacy of topical mometasone furoate with other topical corticosteroids. *Australas J Dermatol*. 2018;59(3):e168–74. <https://doi.org/10.1111/ajd.12762>.
6. Qi QM, Duffy M, Curreri AM, Balkaran JPR, Tanner EEL, Mitragotri S. Comparison of Ionic Liquids and Chemical Permeation Enhancers for Transdermal Drug Delivery. *Adv Funct Mater*. 2020;30(45). <https://doi.org/10.1002/adfm.202004257>.
7. Ruan J, Liu C, Wang J, Zhong T, Quan P, Fang L. Efficacy and safety of permeation enhancers: A kinetic evaluation approach and molecular mechanism study in the skin. *Int J Pharm*. 2022;626. <https://doi.org/10.1016/j.ijpharm.2022.122155>.
8. Xu W, Liu C, Zhang Y, Quan P, Yang D, Fang L. An investigation on the effect of drug physicochemical properties on the enhancement strength of enhancer: The role of drug-skin-enhancer interactions. *Int J Pharm*. 2021;607. <https://doi.org/10.1016/j.ijpharm.2021.120945>.
9. Djekic L, Marković B, Micov A, Tomić M, Pecikoza U, Stepanović-Petrović R. Percutaneous delivery of levetiracetam as an alternative to topical nonsteroidal anti-inflammatory drugs: formulation development, in vitro and in vivo characterization. *Drug Delivery and Translational Research*. 2020;11(1):227–41. <https://doi.org/10.1007/s13346-020-00787-4>.
10. Khattak RZ, Nawaz A, Alnuwaiser MA, Latif MS, Rashid SA, Khan AA, Alamoudi SA. Formulation, In Vitro Characterization and Antibacterial Activity of Chitosan-Decorated Cream Containing Bacitracin for Topical Delivery. *Antibiotics*. 2022;11(9). <https://doi.org/10.3390/antibiotics11091151>.

11. Li Q, Wan X, Liu C, Fang L. Investigating the role of ion-pair strategy in regulating nicotine release from patch: Mechanistic insights based on intermolecular interaction and mobility of pressure sensitive adhesive. *Eur J Pharm Sci.* 2018;119:102–11. <https://doi.org/https://doi.org/10.1016/j.ejps.2018.04.008>.
12. Kamal NS, Krishnaiah YSR, Xu X, Zidan AS, Raney S, Cruz CN, Ashraf M. Identification of critical formulation parameters affecting the in vitro release, permeation, and rheological properties of the acyclovir topical cream. *Int J Pharm.* 2020;590:119914. <https://doi.org/https://doi.org/10.1016/j.ijpharm.2020.119914>.
13. Dong L, Liu C, Cun D, Fang L. The effect of rheological behavior and microstructure of the emulgels on the release and permeation profiles of Terpinen-4-ol. *Eur J Pharm Sci.* 2015;78:140–50. <https://doi.org/10.1016/j.ejps.2015.07.003>.
14. Sun Y, Liu C, Ren S, Zhang Y, Ruan J, Fang L. Combination of ion-pair strategy and chemical enhancers for design of dexmedetomidine long-acting patches: Dual action mechanism induced longer controlled release and better delivery efficiency. *Eur J Pharm Biopharm.* 2023;183:47–60. <https://doi.org/10.1016/j.ejpb.2022.12.014>.
15. Zhang S, Liu C, Yang D, Ruan J, Luo Z, Quan P, Fang L. Mechanism insight on drug skin delivery from polyurethane hydrogels: Roles of molecular mobility and intermolecular interaction. *Eur J Pharm Sci.* 2021;161:105783. <https://doi.org/https://doi.org/10.1016/j.ejps.2021.105783>.
16. Kim YE, Choi SW, Kim MK, Nguyen TL, Kim J. Therapeutic Hydrogel Patch to Treat Atopic Dermatitis by Regulating Oxidative Stress. *Nano Lett.* 2022;22(5):2038–47. <https://doi.org/10.1021/acs.nanolett.1c04899>.
17. Olejnik A, Goscianska J, Nowak I. Active Compounds Release from Semisolid Dosage Forms. *J Pharm Sci.* 2012;101(11):4032–45. <https://doi.org/10.1002/jps.23289>.
18. Zhao H, Liu C, Yang D, Wan X, Shang R, Quan P, Fang L. Molecular mechanism of ion-pair releasing from acrylic pressure sensitive adhesive containing carboxyl group: Roles of doubly ionic hydrogen bond in the controlled release process of bisoprolol ion-pair. *J Controlled Release.* 2018;289:146–57. <https://doi.org/10.1016/j.jconrel.2018.09.024>.
19. Praça FSG, Medina WSG, Eloy JO, Petrilli R, Campos PM, Ascenso A, Bentley MVLB. Evaluation of critical parameters for in vitro skin permeation and penetration studies using animal skin models. *Eur J Pharm Sci.* 2018;111:121–32. <https://doi.org/https://doi.org/10.1016/j.ejps.2017.09.034>.
20. Cheung S, Subbaraman LN, Ngo W, Jay GD, Schmidt TA, Jones L. Localization of full-length recombinant human proteoglycan-4 in commercial contact lenses using confocal microscopy. *J Biomater Sci Polym Ed.* 2019;31(1):110–22. <https://doi.org/10.1080/09205063.2019.1678454>.
21. Corbe E, Laugel C, Yagoubi N, Baillet A. Role of ceramide structure and its microenvironment on the conformational order of model stratum corneum lipids mixtures: an approach by FTIR spectroscopy. *Chem Phys Lipids.* 2007;146(2):67–75. <https://doi.org/https://doi.org/10.1016/j.chemphyslip.2006.12.010>.

22. Horita D, Hatta I, Yoshimoto M, Kitao Y, Todo H, Sugibayashi K. Molecular mechanisms of action of different concentrations of ethanol in water on ordered structures of intercellular lipids and soft keratin in the stratum corneum, *Biochimica et Biophysica Acta (BBA) - Biomembr.* 2015;1848(5):1196–202. <https://doi.org/10.1016/j.bbamem.2015.02.008>.
23. Zeng C, Feng S. Optimized Extraction of Polysaccharides from *Bergenia emeiensis* Rhizome, Their Antioxidant Ability and Protection of Cells from Acrylamide-induced Cell Death. *Plants.* 2020;9(8). <https://doi.org/10.3390/plants9080976>.
24. Fan Z, Cheng P, Zhang P, Gao Y, Zhao Y, Liu M, Gu J, Wang Z, Han J. A novel multifunctional Salecan/ $\kappa$ -carrageenan composite hydrogel with anti-freezing properties: Advanced rheology, thermal analysis and model fitting. *Int J Biol Macromol.* 2022;208:1–10. <https://doi.org/10.1016/j.ijbiomac.2022.03.054>.
25. Xiao Q, Chen G, Zhang Y-H, Chen F-Q, Weng H-F, Xiao A-F. Agarose Stearate-Carbomer940 as Stabilizer and Rheology Modifier for Surfactant-Free Cosmetic Formulations. *Mar Drugs.* 2021;19(6). <https://doi.org/10.3390/md19060344>.
26. Aben S, Holtze C, Tadros T, Schurtenberger P. Rheological Investigations on the Creaming of Depletion-Flocculated Emulsions. *Langmuir.* 2012;28(21):7967–75. <https://doi.org/10.1021/la300221m>.
27. Liu C, Quan P, Li S, Zhao Y, Fang L. A systemic evaluation of drug in acrylic pressure sensitive adhesive patch in vitro and in vivo: The roles of intermolecular interaction and adhesive mobility variation in drug controlled release. *J Controlled Release.* 2017;252:83–94. <https://doi.org/https://doi.org/10.1016/j.jconrel.2017.03.003>.
28. Tang R, Samouillan V, Dandurand J, Lacabanne C, Lacoste-Ferre MH, Bogdanowicz P, Bianchi P, Villaret A, Nadal-Wollbold F. Identification of ageing biomarkers in human dermis biopsies by thermal analysis (DSC) combined with Fourier transform infrared spectroscopy (FTIR/ATR). *Skin Res Technol.* 2017;23(4):573–80. <https://doi.org/10.1111/srt.12373>.
29. Kováčik A, Kopečná M, Vávrová K. Permeation enhancers in transdermal drug delivery: benefits and limitations. *Expert Opin Drug Deliv.* 2020;17(2):145–55. <https://doi.org/10.1080/17425247.2020.1713087>.
30. Liu Y, Liu C, Jia W, Xu W, Quan P, Fang L. The Molecular Mechanism of Propylene Glycol Monocaprylate on Skin Retention: Probing the Dual Roles on the Molecular Mobility and Collagen Connection in Roflumilast Cream. *AAPS PharmSciTech.* 2022;23(5). <https://doi.org/10.1208/s12249-022-02284-y>.
31. Yang D, Liu C, Quan P, Fang L. A systematic approach to determination of permeation enhancer action efficacy and sites: Molecular mechanism investigated by quantitative structure – activity relationship. *J Controlled Release.* 2020;322:1–12. <https://doi.org/10.1016/j.jconrel.2020.03.014>.

## Figures

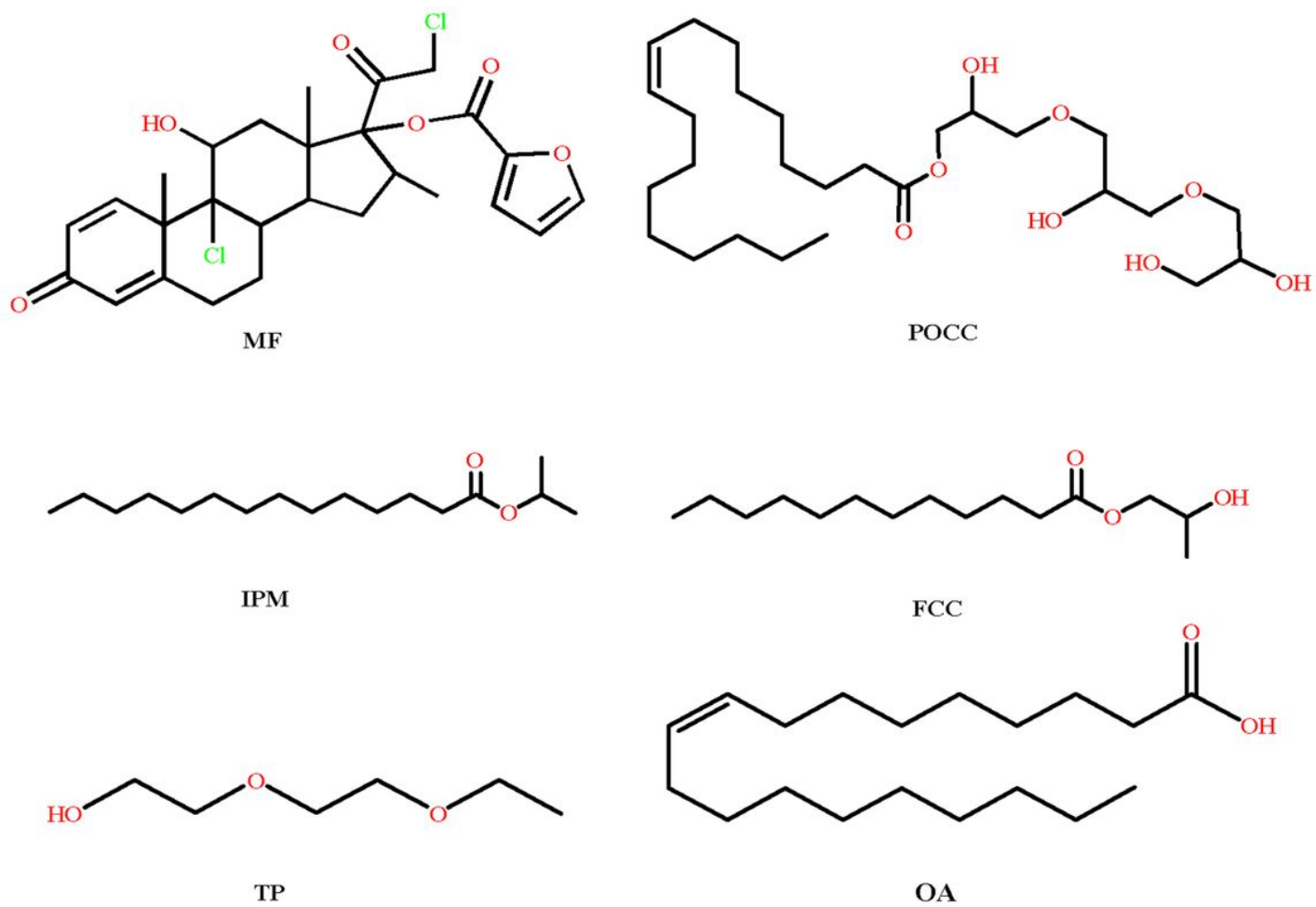


**Figure 1**

The chemical structures of mometasone furoate (MF) and permeation enhancers in formulations



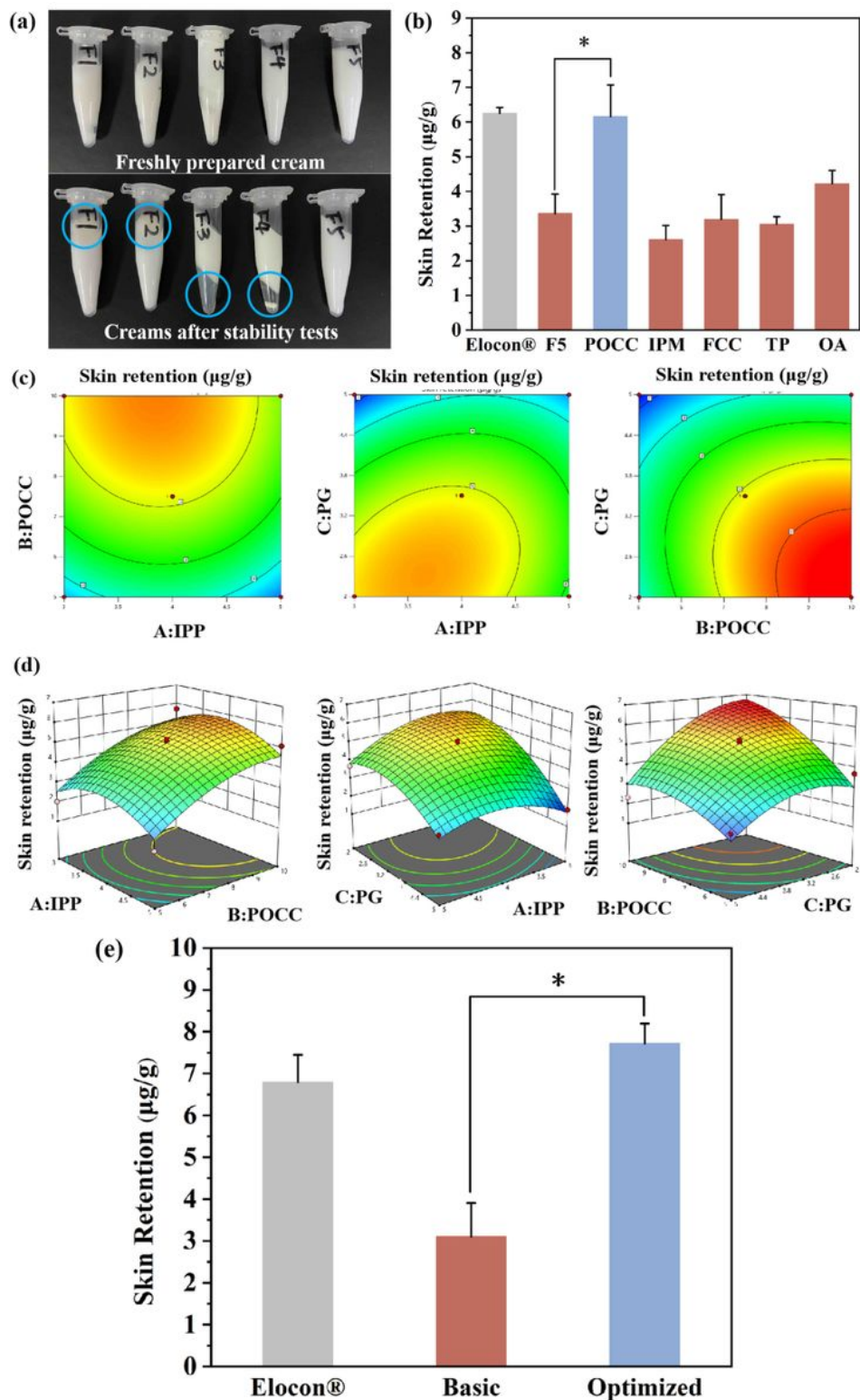


**Figure 2**

(a) Appearance of the cream after preparation and stability testing (b) The skin retention of MF creams containing different kinds of chemical permeation enhancers ( $n = 4$  \* $p < 0.05$  vs. F5). (c) The 2D response surface plots and (d) The 3D response surface plots showing the effect of interactions between IPP-POCC, IPP-PG, and POCC-PG on the characteristics of the MF creams (e) Validation of predicted formulations ( $n=4$ ).

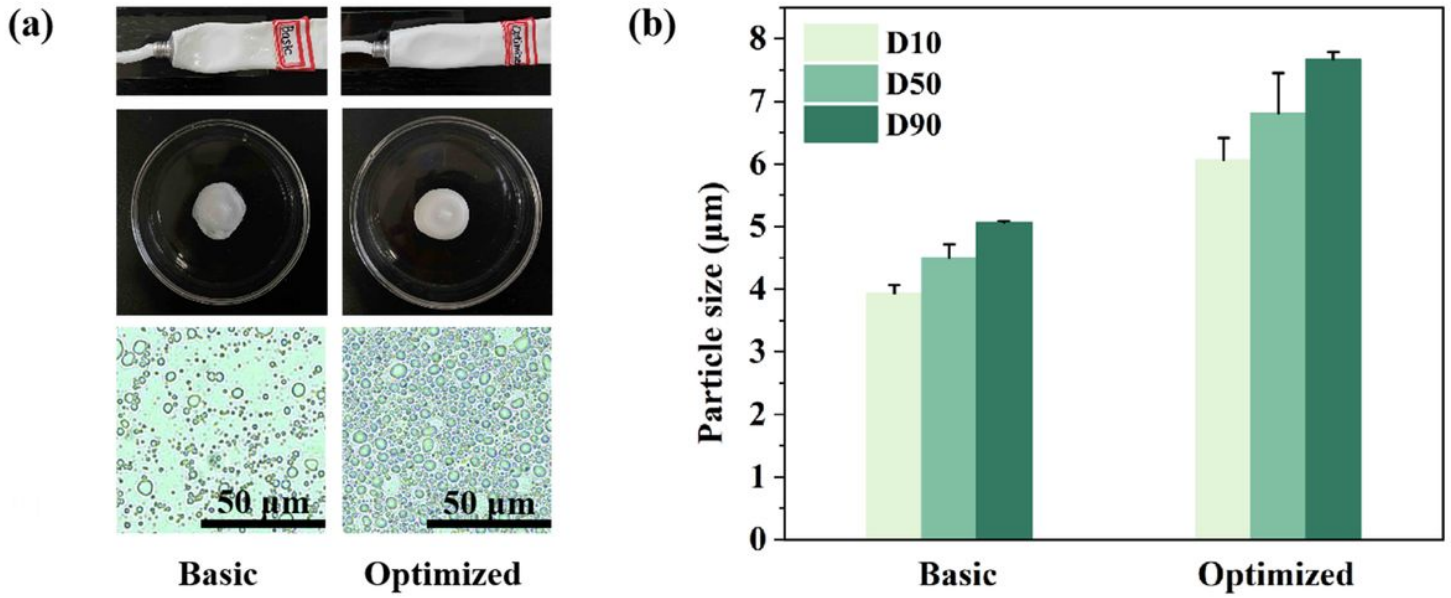


**Figure 3**

(a) Appearance and microscopic properties of the creams (b) Particle size measurement of creams ( $n = 3$ )

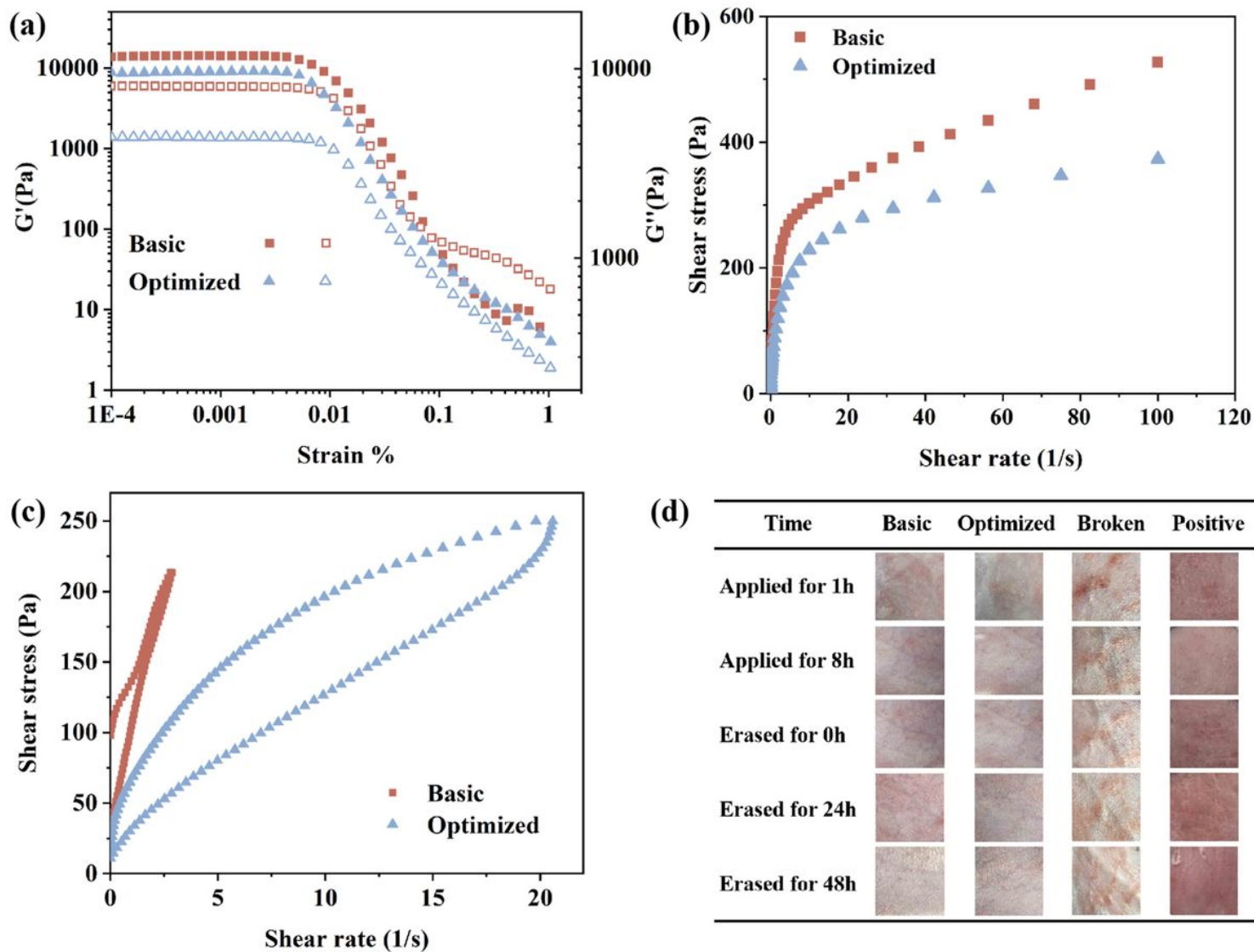


**Figure 4**

(a) Strain sweep of the creams (b) Flow characterization of the creams (c) Thixotropic cycle of the creams ( $n=3$ ) (d) Pictures of skin irritation experiment.

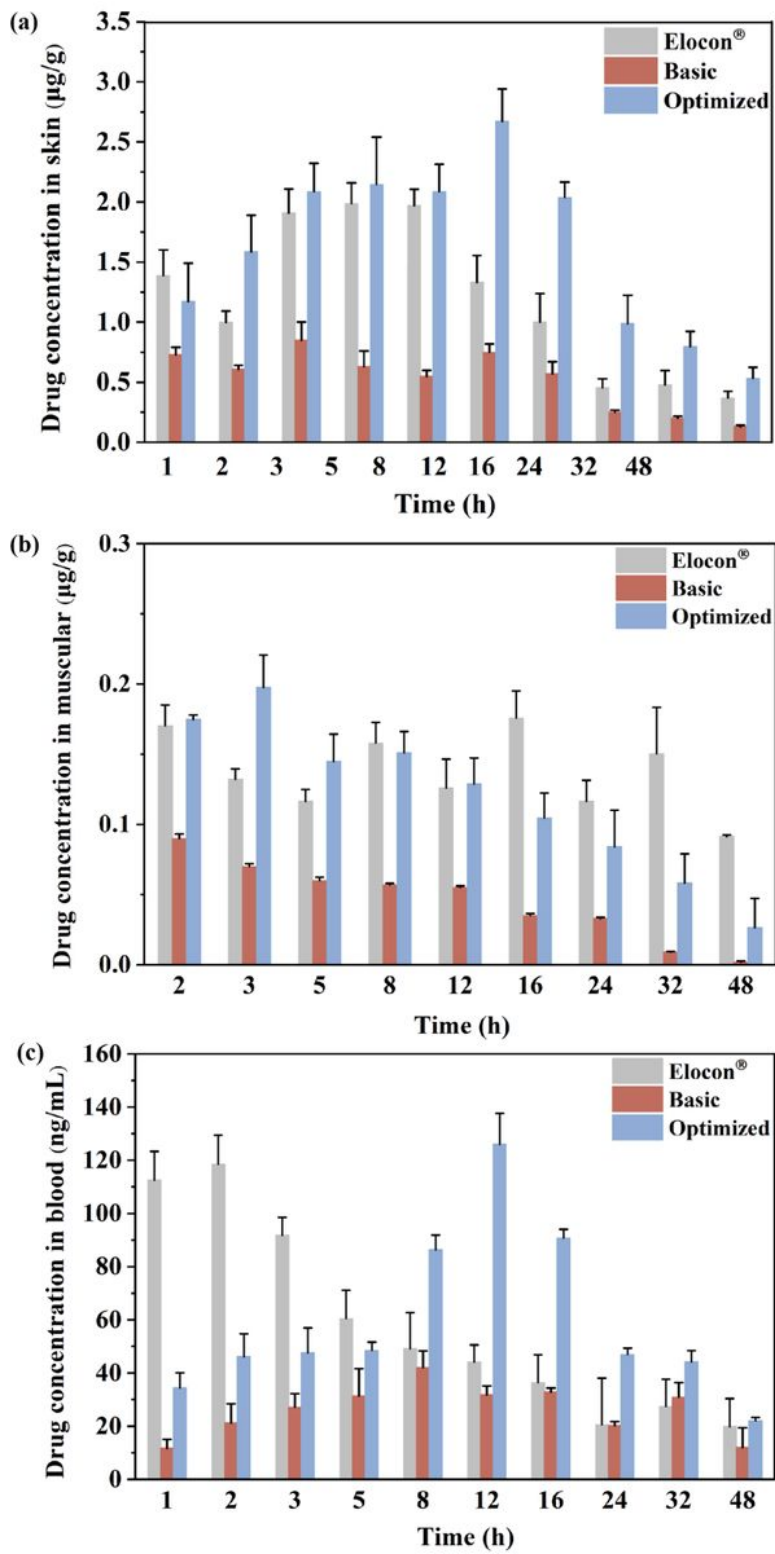


**Figure 5**

*In vivo* tissue distribution study of MF in (a) skin, (b) muscle, and (c) blood ( $n= 6$ )

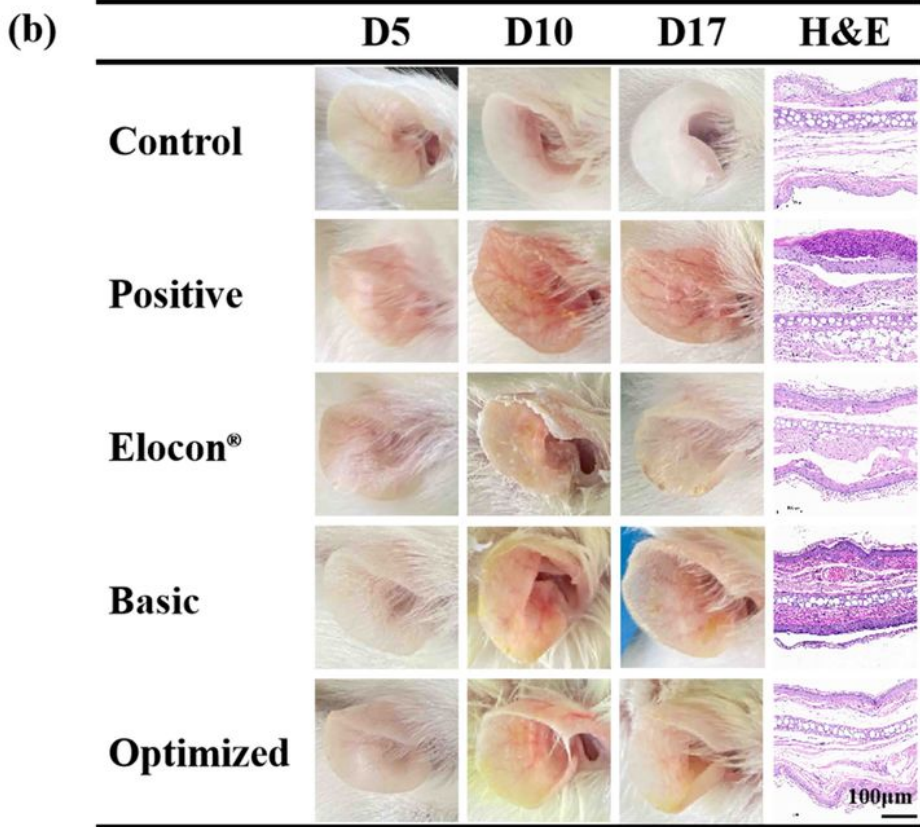
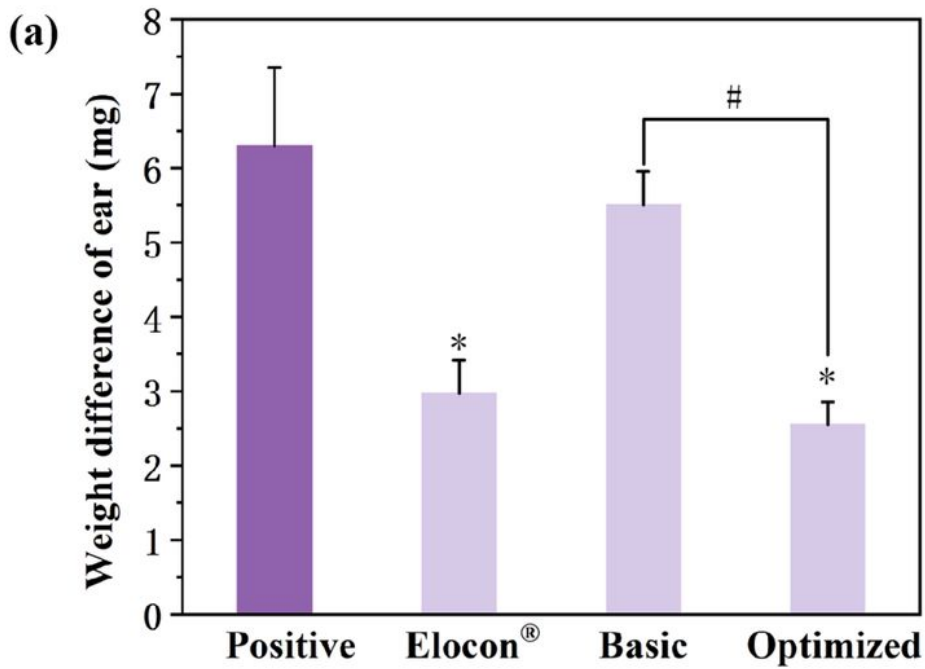


**Figure 6**

(a) Representative photographs of the right ear skin of each group after treatment and histological photographs of the right ear skin sections of mice stained by H&E after treatment. (b) Ear weight difference. ( $n = 6$ , \* $p < 0.05$  vs. positive group # $p < 0.05$  vs. optimized group)

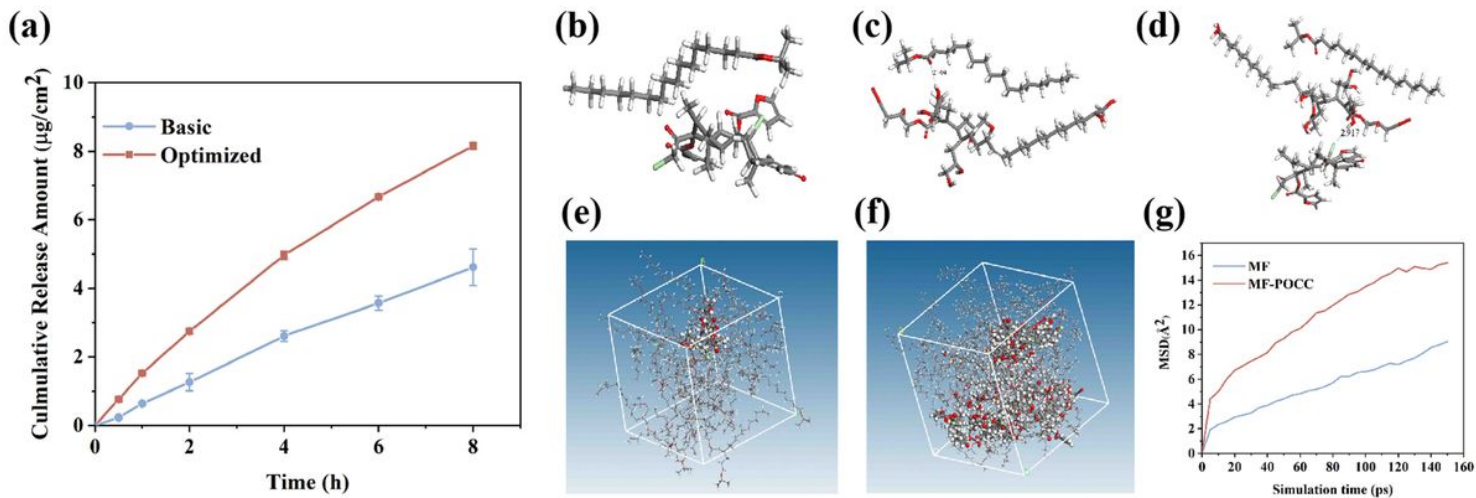


Figure 7

(a) MF release profile in the basic and optimized formulations ( $n=4$ ) Snapshots of (b) IPP-MF, (c) IPP-POCC, (d) IPP-MF-POCC with the minimum energy, (e) MF+IPP and (f) MF-POCC+IPP system at the end of molecular dynamic simulation and (g) the mean square displacement (MSD) of MF and MF-POCC in IPP.

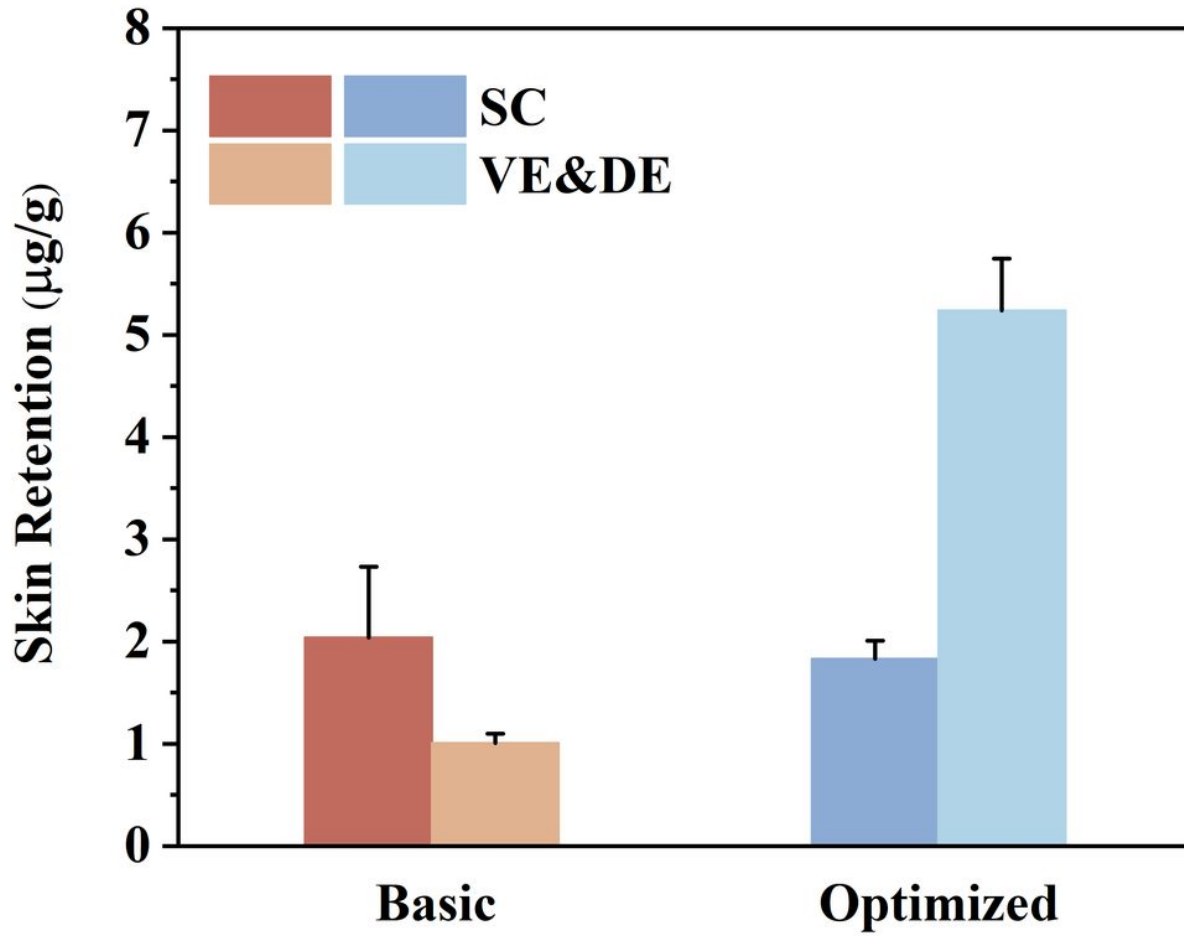


Figure 8

The amount of MF in SC layer and VE&DE layer ( $n=4$ )

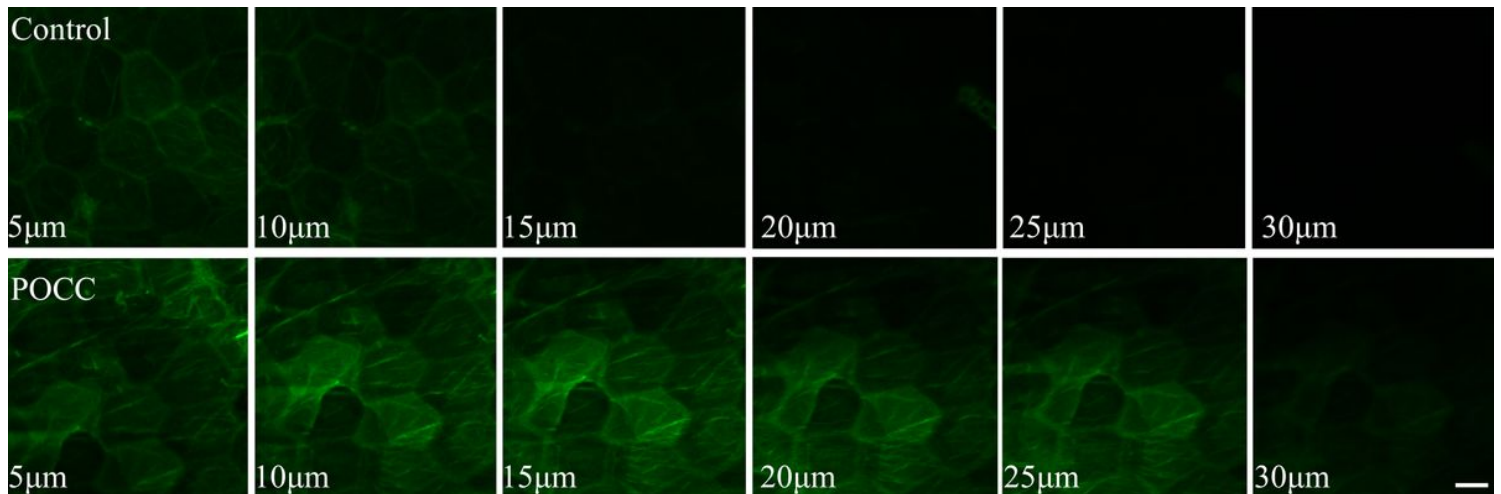
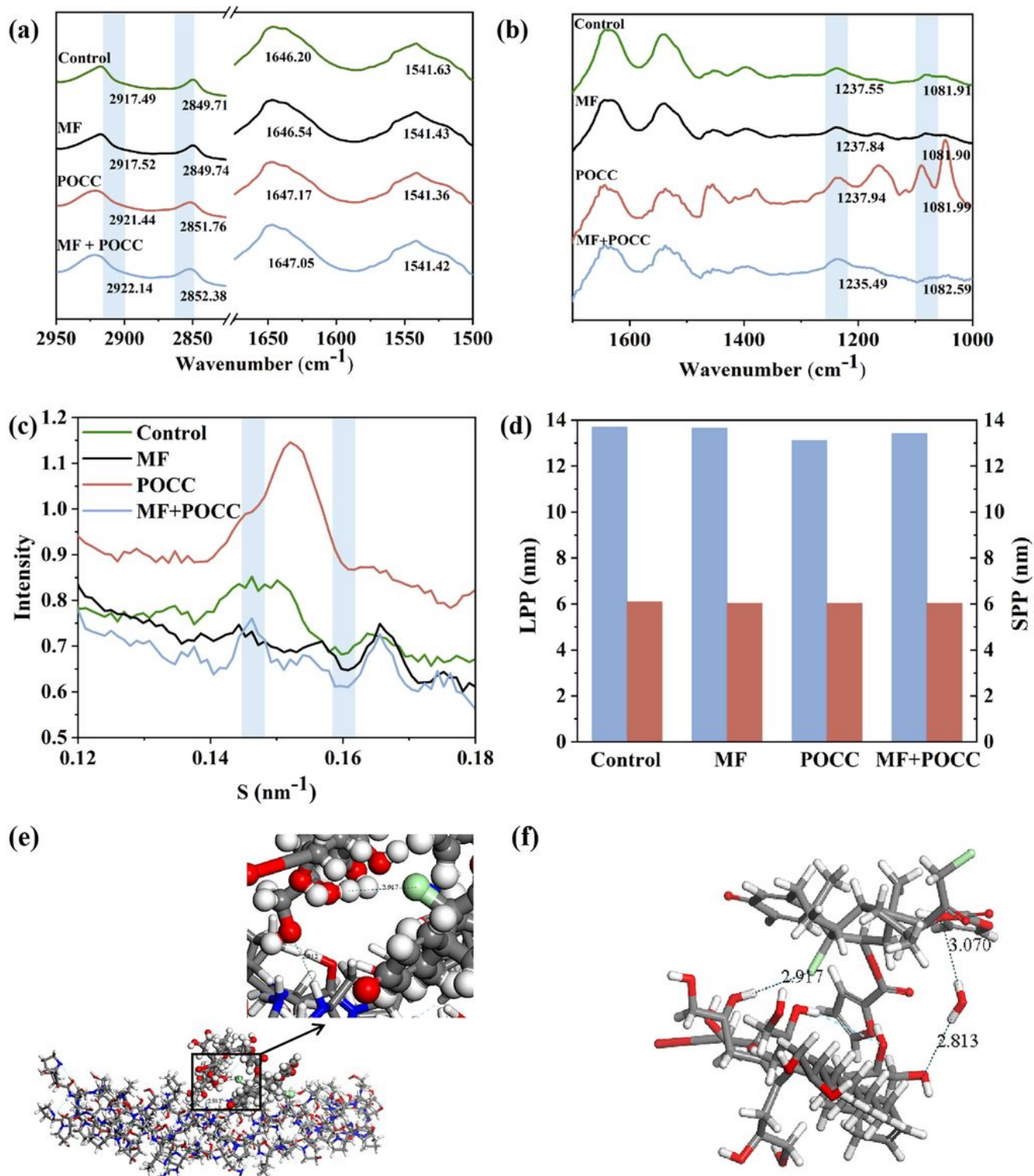


Figure 9

Confocal laser scanning microscopy images of different depths of the skin treated by FITC and POCC (scale bar represented 10  $\mu\text{m}$ ).



**Figure 10**

The ATR-FTIR spectra of (a) SC and (b) VE/DE samples after the treatment of ethanol solutions with the help of de-convolution. (c) Small-angle X-ray diffraction profiles of SC. (d) The Repeat Distance of SC



Obtained from the 2nd-Order Diffraction Peak for the Long Lamellar Structure and the 1st-Order Diffraction Peak for the Short Lamellar Structure. Minimum energy complexes of (e) POCC-MF with COL, (f) POCC-MF with H<sub>2</sub>O.

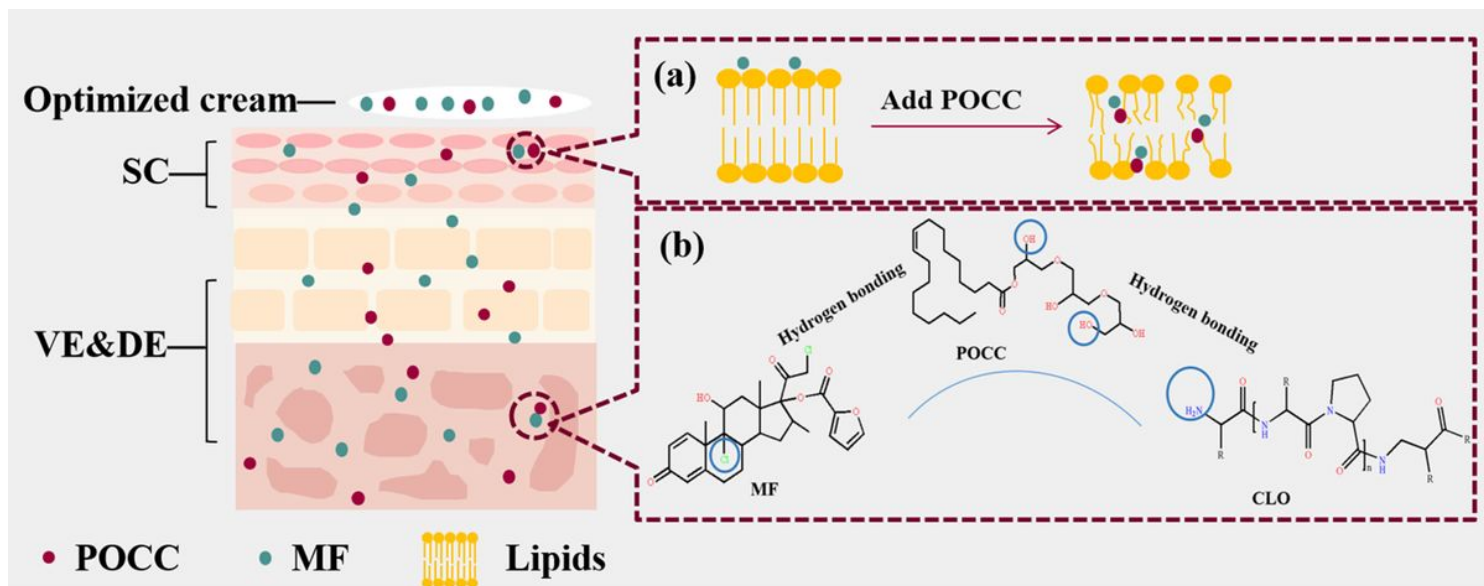


Figure 11

Promoting molecular interactions between MF POCC and skin during retention

## Supplementary Files

This is a list of supplementary files associated with this preprint. Click to download.

- [GA.png](#)